An experimental determination of $g_J(^4\mathrm{He},2\,^3S_1)/g_J(^1\mathrm{H},1\,^2S_{1/2})$‡

G. M. Keiser† and H. G. Robinson
Physics Department, Duke University, Durham, North Carolina 27706

C. E. Johnson
Physics Department, North Carolina State University, Raleigh, North Carolina 27607

(Received 28 April 1977)

The ratio of the g_J factor of $^4\mathrm{He}(2\,^3S_1)$ to that of $^{87}\mathrm{Rb}(5\,^2S_{1/2})$ has been measured to a fractional accuracy of $\pm 5\times 10^{-8}$. The Rb atoms were optically pumped, and the $^4\mathrm{He}(2\,^3S_1)$ Zeeman resonance was observed through a combination of spin-exchange collisions and spin-dependent Penning ionization. Linewidths as narrow as 220 Hz were observed for the $^4\mathrm{He}(2\,^3S_1)$ Zeeman resonance. The accuracy of this experiment was limited by a systematic shift in the He g_J factor that depended upon the intensity of the discharge used to excite the He atoms to the $2\,^3S_1$ state. Calculations indicate that transfer of coherence in spin-exchange collisions with free electrons contributes to this shift. The measured ratio $g_J(^4\mathrm{He},2\,^3S_1)/g_J(^{87}\mathrm{Rb},5\,^2S_{1/2}) = 1-46.798(50)\times 10^{-6}$. Using the previously measured ratio of the g_J factors of the ground state of rubidium to the ground state of hydrogen, we determine the ratio $g_J(^4\mathrm{He},2\,^3S_1)/g_J(^1\mathrm{H},1\,^2S_{1/2}) = 1-23.214(50)\times 10^{-6}$. This result agrees with recent theoretical calculations and experimental determinations using atomic-beam techniques, but disagrees with an earlier experimental determination using optical-pumping techniques.

I. INTRODUCTION

Measurements of the electronic g factors of simple atomic systems have provided a means of checking the theoretical predictions of relativistic quantum mechanics and quantum electrodynamics as well as the dynamics of several-particle systems in magnetic fields. Since the theoretical corrections to the electronic g factors differ from the predictions of the nonrelativistic theory by terms which may be expressed as a power series in the fine-structure constant α and the ratio of the electron mass to the nuclear mass m/M, experimental verification of the small higher-order corrections to the electronic g factor has placed severe demands on experimental techniques. Nevertheless, it has been possible to compare experiment and theory to a fractional accuracy of 10^{-11} for the ratio of the electronic g factors of hydrogen and deuterium,[1] and 10^{-8} for the ratio of the electronic g factor of hydrogen to that of the free electron.[2] In these cases, the agreement between theory and experiment is excellent. However, in general for many-electron atoms, inaccuracies in the atomic wave functions limit the accuracy of theoretical calculations.[3-5] One exception is the case of the helium atom where extremely accurate variational wave functions are available[6]; a comparison of experimental results with the theoretical calculations provides a valid test of the theory for multielectron atoms.

This paper describes a measurement of the ratio

$$R\equiv\frac{g_J(^4\mathrm{He},2^3S_1)}{g_J(^{87}\mathrm{Rb},5^2S_{1/2})}.$$

Using the experimentally determined ratio of the electronic g factor of rubidium in its ground state to that of hydrogen in its ground state,[7] we have

$$R'\equiv\frac{g_J(^4\mathrm{He},2^3S_1)}{g_J(^1\mathrm{H},^2S_{1/2})}=\frac{g_J(^4\mathrm{He})}{g_J(^{87}\mathrm{Rb})}\times\frac{g_J(^{87}\mathrm{Rb})}{g_J(^1\mathrm{H})}$$

as the quantity which may be compared with theoretical calculations.[8,9] A preliminary account of our work was published earlier.[10]

Drake, Hughes, Lurio, and White[11] first measured R' using an atomic beam technique in 1958. Their result agreed with the calculation of Perl and Hughes[12] who included relativistic corrections to the $^4\mathrm{He}(2^3S_1)$ g_J factor to order α^2. In 1972, Leduc, Laloë, and Brossel[13] measured the ratio of the electronic g factor of $^4\mathrm{He}(2^3S_1)$ to nuclear g factor of the ground state of ^{3}He. Using two other experimentally determined ratios,[14,15] they obtained the ratio R'. This result was in mild disagreement with earlier work and stimulated additional interest. Grotch and Hegstrom[9] and Lewis and Hughes[8] calculated the bound-state corrections to the Schwinger moment[16] of order α^3 and the nuclear-mass corrections of order $\alpha^2 m/M$ to the g_J factor of $^4\mathrm{He}(2^3S_1)$ and found that these higher-order corrections could not account for the disagreement. A more accurate atomic-beam experiment by Aygün, Zak, and Shugart[17] agreed with the previous atomic-beam experiment and with the theoretical calculations but clearly disagreed with the optical-pumping experiment. This provided the motivation for our effort to make a second high-precision optical-pumping determination to resolve the discrepancy between the experimental

values.

This paper is divided into six sections. Sections II and III describe the apparatus and the various contributions to the helium and rubidium Zeeman linewidths as well as possible contributions to asymmetries in the line shapes and to shifts in the center frequencies. The procedure used is discussed in Sec. IV. The results are presented in Sec. V and are compared with other theoretical and experimental results in the final section.

II. APPARATUS

A. Technique

An outline of the experimental apparatus is shown in Fig. 1. Rubidium atoms in a 30-cm^3 cylindrical Pyrex cell were optically pumped using circularly polarized light from a rubidium resonance lamp. Approximately 10 Torr of helium gas in the cell provided a buffer gas for the rubidium atoms and a source for the $^4He(2^3S_1)$ atoms, which were excited to this metastable state by a pulsed rf discharge. Zeeman magnetic resonance signals were observed at magnetic fields of 50 and 100 G by monitoring the intensity of the light transmitted through the cell. The Zeeman resonance of the $^4He(2^3S_1)$ atoms was detected through a combination of spin-exchange collisions and spin-dependent Penning ionization. Linewidths as narrow as 220 Hz were observed for the $^4He(2^3S_1)$ Zeeman resonance at a field of 100 G.

B. Sample cells

The 30-cm^3 Pyrex cells were evacuated and baked for more than 10 h at a temperature of approximately 375 °C. Pressures measured by an ionization gauge after the cell had cooled to room temperature were typically less than 3×10^{-7} Torr. The walls of the cell were scrubbed by admitting several Torr of helium, exciting an intense 100 MHz discharge, and pumping out the helium while the discharge was running. This scrubbing procedure was repeated with hydrogen and then a number of times with helium until the visible emission spectrum of the discharge showed mainly those spectral lines characteristic of helium and the absence of any broad molecular bands. Multiply distilled isotopically pure (99.2%) ^{87}Rb and research-grade helium, additionally purified by a barium getter, were used to fill the sample cells. Cells were prepared at four different helium pressures.

After initial data had been taken on each of the four cells, they were placed in a nuclear reactor at North Carolina State University and irradiated by a neutron flux of 10^{11} cm^{-2} sec^{-1} for 6 min. The original motivation for irradiating the cells was to make the glass slightly radioactive so that β emission would provide sufficient electron densities within the cell to run a very weak discharge. Immediately after irradiation, the measured activity was approximately 0.1 mC due predominantly to the decay of ^{24}Na. Because of the small cross section for absorption of neutrons by ^4He, the irradiation had a negligible effect on the helium in the sample cell. The number of ^{88}Sr atoms created through neutron absorption by ^{87}Rb and the subsequent decay of ^{88}Rb into ^{88}Sr is estimated to be 6×10^7, too small to have a significant effect. The stable isotopes ^{30}Si and ^{41}K and the long-lived ^{40}K created would have a negligible effect on the glass structure. After a week the β emission had essentially disappeared, although the glass retained a brown tint as a result of the irradiation. Nevertheless, the discharge in the four cells continued to operate at significantly lower voltages than before irradiation. Apparently the properties of the glass had been altered, allowing a weaker discharge.

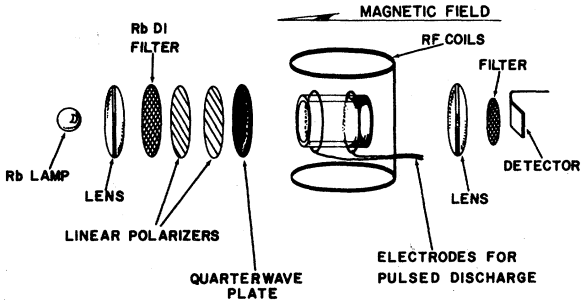

FIG. 1. Experimental apparatus. Optical-pumping light from the Rb lamp is filtered and circularly polarized before passing through the sample cell containing ground-state ^{87}Rb atoms and $^4He(2^3S_1)$ atoms, which are produced by a pulsed discharge. Zeeman resonances induced by an oscillating rf field are observed by detecting changes in the transmitted light intensity.

C. Pulsed rf discharge

A 50-MHz discharge was used to excite the helium atoms from the ground state to the 2^3S_1 state and was driven by two helical wire electrodes wound around opposite ends of the cylindrical sample cell. The axis of the cell was parallel to the direction of the static magnetic field. By pulsing the discharge, its average intensity could be substantially decreased. If the plasma was allowed to completely disappear before repulsing, significantly higher oscillator plate voltages were required, which consequently resulted in a

stronger average discharge. The transition from a very weak plasma to the complete disappearance of the plasma was abrupt and is believed to be associated with the change from ambipolar to free diffusion. The discharge was typically on for 50 μsec at a pulse rate of 240 Hz. The rate was adjustable by integral multiples of 30 Hz to suppress beats with the lock-in reference frequency of 2.5 Hz.

D. Magnetic field

A description of our solenoid and field-stabilization system has already been given.[18] In addition to magnetic field correction coils designed to produce Legendre-polynomial gradients, this experiment utilized coils which produced the lowest-order nonaxially symmetric associated Legendre-polynomial gradients.[19] The fractional inhomogeneity of the magnetic field over the sample cell was measured to be less than 1×10^{-7}. The field was locked to a stable oscillator via a rubidium magnetometer so that the fractional long-term drift of the magnetic field was less than 1×10^{-8}/h.

E. Data acquisition system

Data were acquired by an automated system which programmed a frequency synthesizer, measured the analog response (i.e., the optical-pumping signal) via a phase-sensitive detector, and punched the digitized output on paper tape. The phase-sensitive detector was of special design[20] to reduce distortions in line shape due to transient or phase-shift effects. The rf used to induce Zeeman transitions was square-wave amplitude modulated by a relay driven at 2.5 Hz. During each clock half-cycle, the detector waited for a predetermined interval to allow any transient signal to die out before integration was enabled. Both rf-on and rf-off integrated outputs were available; the differential signal was digitized by a Hewlett-Packard model 2212A voltage-to-frequency converter and a Hewlett-Packard 5245L counter. During the first two clock cycles the frequency synthesizer was programmed to a new frequency and the counter output corresponding to the previous frequency was punched on paper tape. At the end of the second clock cycle, the counter was enabled and counted for a present time of 4, 6, or 12 clock cycles. This completed one cycle of the data-acquisition system.

III. LINEWIDTHS, CENTER FREQUENCIES, AND LINE SHAPES

Zeeman resonances of the 2^3S_1 state of helium have usually been observed in optical-pumping

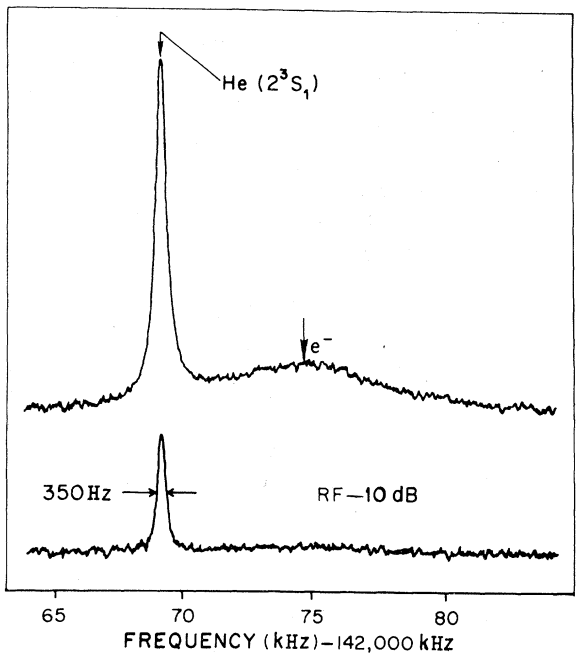

FIG. 2. Helium 2^3S_1 and free-electron Zeeman resonances at 50 G. The e^- resonance is barely observed when the rf power is reduced by 10 dB; data were taken with the rf reduced even further.

experiments by pumping the 2^3S_1 state with light resonant at the $2^3S_1 \rightarrow 2^3P_J$ transitions.[21,22] We observed this Zeeman resonance, however, through a combination of spin-dependent Penning ionization and spin-exchange collisions where the optically pumped species was ground-state ^{87}Rb atoms. Polarization of the ^{4}He(2^3S_1) atoms by spin-exchange is possible either through collisions between Rb and He atoms or collisions in which free electrons act as an intermediary. Observing the ^{4}He(2^3S_1) Zeeman resonance while pumping Rb produced substantially narrower He linewidths and, in addition, allowed simultaneous observation of the free-electron Zeeman resonance. Although the g_J factors of the free electron and the ^{4}He(2^3S_1) atoms differ by only about 40 ppm, these two resonances are well resolved at a field of 50 G, as shown in Fig. 2. The dominant processes present in the sample cell and their effects on the Zeeman linewidths, center frequencies, and line shapes are now discussed.

A. Spin-exchange collisions

The effects of spin-exchange collisions between free electrons and rubidium atoms was first studied by Balling, Hanson, and Pipkin,[23] who measured the broadening of the electron resonance and the shift in its center frequency due to spin-ex-

change collisions with ground-state rubidium atoms. For certain experimental conditions, the free-electron polarization and density are often considerably smaller than the rubidium polarization and density. Therefore, the corresponding broadening and shift in the ground-state rubidium Zeeman transitions have been more difficult to observe. Taking into account the effects of nuclear spin, Grossetête[24,25] has shown that in the low-field limit, these collisions broaden the rubidium $(F, m_F) \rightarrow (F, m_F - 1)$ resonance by an amount

$$\Delta f_{\mathrm{Rb}} = \left(\frac{3}{4} - \frac{m_F^2 - m_F}{4F^2}\right) \frac{1}{\pi}\, n_e \sigma_{e\,\mathrm{Rb}} v\,, \tag{1}$$

where n_e is the electron number density, $\sigma_{e\,\mathrm{Rb}}$ is the electron-rubidium spin-exchange cross section, and v is the relative velocity of the electrons and rubidium atoms. The shift in each of the rubidium Zeeman transitions due to spin exchange is

$$\delta\nu_{\mathrm{Rb}} = (1/8\pi) K P(e) n_e \sigma_{e\,\mathrm{Rb}} v\,, \tag{2}$$

where $P(e)$ is the electron polarization and K is a constant which depends on the singlet and triplet partial-wave-scattering amplitudes. From these two equations, the ratio of the shift in the transition frequency to the broadening is

$$\frac{\delta\nu_{\mathrm{Rb}}}{\Delta f_{\mathrm{Rb}}} = \frac{KP(e)}{8[\frac{3}{4} - (m_F - m_F^2/4F^2)]}\,. \tag{3}$$

Since the sign of the frequency shift depends on the direction of the electron polarization with respect to the static magnetic field, these shifts may be experimentally corrected at low magnetic fields by measuring the rubidium Zeeman transition frequencies with the electron polarization parallel and antiparallel to the static magnetic field.

Happer and Tang[26] demonstrated that transfer of coherence in spin-exchange collisions could shift the resonant frequencies and change the relaxation rates of Zeeman resonances. These effects only occur when the difference in the Larmor precession frequency of the two resonances is the same order of magnitude as, or less than, the spin-exchange rates. They observed a shift in the ground-state rubidium Zeeman resonances and a dramatic reduction in the linewidth of the single observable resonance at high spin-exchange rates. Dupont-Roc, Leduc, and Laloë[27] have pointed out that a similar effect should occur for $^3\mathrm{He}(2^3S_1)$ Zeeman resonances at very low magnetic fields.

In this experiment, the free electron and the $^4\mathrm{He}(2^3S_1)$ Zeeman resonances are separated by approximately 6 kHz at a magnetic field of 50 G. Spin-exchange collisions between these two species are estimated to make significant contributions to the 5-kHz electron linewidth and the 300-Hz helium linewidth. Although these resonances are resolved, they are not sufficiently well separated that the effects of transfer of coherence in spin-exchange collisions can be neglected. A detailed calculation of the effects of spin-exchange collisions between free electrons and $^4\mathrm{He}(2^3S_1)$ atoms has been given.[28] Some of the more important results are discussed here.

The effects of these spin-exchange collisions may be adequately represented in the limit of low polarization by the differential equations

$$\frac{d\langle\vec{S}_e\rangle}{dt} = \frac{1}{T_{ee}}\left(\tfrac{1}{2}\langle\vec{S}_h\rangle - \tfrac{4}{3}\langle\vec{S}_e\rangle\right) + \frac{K'}{T_{ee}}\left(\langle\vec{S}_e\rangle \times \langle\vec{S}_h\rangle\right), \tag{4}$$

$$\frac{d\langle\vec{S}_h\rangle}{dt} = \frac{1}{T_{eh}}\left(\tfrac{4}{3}\langle\vec{S}_e\rangle - \tfrac{1}{2}\langle\vec{S}_h\rangle\right) + \frac{K'}{T_{eh}}\left(\langle\vec{S}_h\rangle \times \langle\vec{S}_e\rangle\right). \tag{5}$$

Here, the brackets $\langle\ \rangle$ indicate an average over the ensemble of atoms and electrons: $\langle\vec{S}_e\rangle$ is the average of the expectation value of the spin of the free electrons, while $\langle\vec{S}_h\rangle$ is the average of the expectation value for the helium 2^3S_1 atoms. The spin-exchange rate for an electron with helium 2^3S_1 atoms is $1/T_{ee}$, and the spin-exchange rate for the metastable helium atom with electrons is $1/T_{eh}$. The constant K' is determined by the doublet and quartet scattering amplitudes. In the absence of other influences, the vectors $\langle\vec{S}_e\rangle$ and $\langle\vec{S}_h\rangle$ will precess about one another and relax until $\langle\vec{S}_e\rangle = \frac{3}{8}\langle\vec{S}_h\rangle$.

The effects of spin-exchange collisions on the magnetic resonance signals may be calculated by including the above relations in Bloch's equations.[29] Written in terms of $\langle\vec{S}_e\rangle$ and $\langle\vec{S}_h\rangle$, the complete equations, in a reference frame rotating at angular velocity $\vec{\omega}$, are

$$\begin{aligned}\frac{d\langle\vec{S}_e\rangle}{dt} &= \langle\vec{S}_e\rangle \times \left(\gamma_e \vec{H} + \frac{K'}{T_{ee}}\langle\vec{S}_h\rangle + \vec{\omega}\right) \\ &\quad + \frac{1}{T_{ee}}\left(\tfrac{1}{2}\langle\vec{S}_h\rangle - \tfrac{4}{3}\langle\vec{S}_e\rangle\right) + \frac{1}{T_{1e}}\left(\langle S_e\rangle_0 - \langle S_e\rangle_z\right)\hat{z} \\ &\quad - \frac{1}{T_{2e}}\left(\langle S_e\rangle_x \hat{x} + \langle S_e\rangle_y \hat{y}\right),\end{aligned} \tag{6}$$

$$\begin{aligned}\frac{d\langle\vec{S}_h\rangle}{dt} &= \langle\vec{S}_h\rangle \times \left(\gamma_h \vec{H} + \frac{K'}{T_{eh}}\langle\vec{S}_e\rangle + \vec{\omega}\right) \\ &\quad + \frac{1}{T_{eh}}\left(\tfrac{4}{3}\langle\vec{S}_e\rangle - \tfrac{1}{2}\langle\vec{S}_h\rangle\right) \\ &\quad + \frac{1}{T_{1h}}\left(\langle S_h\rangle_0 - \langle S_h\rangle_z\right)\hat{z} \\ &\quad - \frac{1}{T_{2h}}\left(\langle S_h\rangle_x \hat{x} + \langle S_h\rangle_y \hat{y}\right),\end{aligned} \tag{7}$$

where γ_e and γ_h are the gyromagnetic ratios for the free electron and helium atom, T_{1e} and T_{1h} are the longitudinal relaxation times, and T_{2e} and T_{2h} are the transverse relaxation times. The magnetic field $\vec{H}$ is taken to consist of a large static component $\vec{H}_0$, which lies along the z axis, and a small component $\vec{H}_1$, which lies along the x axis in the rotating reference frame. $\langle S\rangle_0$ is the equilibrium polarization.

From these equations, it can be seen that the term which includes the constant K' has exactly the same effect as an additional magnetic field. It is this term which is the source of the usual spin-exchange frequency shift. The sign of the shift depends on whether the equilibrium values of $\langle \vec{S}_e \rangle$ and $\langle \vec{S}_h \rangle$ are parallel or antiparallel to the static magnetic field. We determined experimentally that the center frequency of the $^4\mathrm{He}(2^3S_1)$ Zeeman resonance was independent of the direction of $\langle \vec{S}_e \rangle$ with respect to the static magnetic field. These results are discussed in Sec. V. Therefore, the constant K' may be set equal to zero, and this term in the equation may be neglected.

Then, Eqs. (6) and (7) become a set of six linear coupled differential equations. In the absence of an oscillating magnetic field $\vec{H}_1$, Happer and Tang[26] have shown that the resonant frequencies and relaxation rates for these two coupled systems may be expressed in terms of two complex eigenvalues. The real parts of these eigenvalues represent relaxation rates, and the complex parts represent the resonant frequencies. For free electrons and $^4\mathrm{He}(2^3S_1)$ atoms, these complex eigenvalues are the two solutions to the secular determinant

$$\begin{vmatrix} \lambda - \omega_e & 1/2T_{ee} \\ 4/3T_{eh} & \lambda - \omega_h \end{vmatrix} = 0 , \tag{8}$$

where ω_e and ω_h are complex quantities,

$$\omega_e = i\omega_{0e} + \frac{1}{T_{2e}} + \frac{4}{3T_{ee}} ,$$
$$\omega_h = i\omega_{0h} + \frac{1}{T_{2h}} + \frac{1}{2T_{eh}} . \tag{9}$$

Here, ω_{0e} and ω_{0h} are the resonant frequencies of the free electrons and the helium atoms in the absence of spin exchange. As the spin-exchange rates increase, the two resonant frequencies shift toward one another. The effects of transfer of coherence in spin-exchange collisions also tend to increase the relaxation rate of the broader resonance and decrease the relaxation rate of the narrower resonance. At very high spin-exchange rates, the relaxation rate of the narrower resonance approaches the average relaxation rate of the free electrons and the helium atoms exclusive of spin exchange.

The line shapes of the magnetic resonance signals may be calculated by finding the eigenvectors associated with these eigenvalues, and solving Eqs. (6) and (7) for equilibrium conditions. It can be shown that the line shape of the helium 2^3S_1 resonance for the case where the electron and helium resonances are sufficiently well resolved, and where the helium resonance is not saturated, is given by[28]

$$S_h(\omega) = \frac{A\omega_1^2[(B_3/T'_{2h}) + B_4(\omega - \omega'_{0h})]}{(\omega - \omega'_{0h})^2 + (1/T'_{2h})^2 + \omega_1^2[(B_3/T'_{2h}) + B_4(\omega - \omega'_{0h})]} , \tag{10}$$

where ω'_{0h} and $1/T'_{2h}$ are the resonant frequency and relaxation rate in the presence of spin exchange. The effects of transfer of coherence in spin-exchange collisions shift the helium resonant frequency toward higher frequencies and decrease the relaxation rate of the helium resonance. Expressions[28] for the constants A, B_3, and B_4 may be calculated if the sensitivity of the detection method and the relaxation and spin-exchange rates are known. The coefficient B_4 determines the amplitude of the dispersion line shape. In the absence of transfer of coherence in spin-exchange collisions, the line shapes are Lorentzian and the coefficient B_4 is equal to zero.

B. Pulsed discharge

Since the discharge was pulsed, the number densities of the atoms, the equilibrium polarization, and the relaxation processes were all periodic functions of time. It is important to determine the effect of the pulsed discharge on the line shape of the Zeeman resonances. A semiclassical argument, based on Bloch's equations, is used.

Neglecting the effects of spin exchange, Bloch's equations in a rotating reference frame may be written

$$\frac{d\langle \vec{S}\rangle}{dt} = \langle \vec{S}\rangle \times (\gamma \vec{H} + \hat{\omega}) + \frac{1}{T_1}(\langle S\rangle_0 - \langle S\rangle_z)\hat{z} - \frac{1}{T_2}(\langle S\rangle_x \hat{x} + \langle S\rangle_y \hat{y}) . \tag{11}$$

The symbols have the same meaning as in Eqs. (6) and (7) but are taken to apply to any of the observed resonances. The relaxation rates, $1/T_1$ and $1/T_2$, and the equilibrium polarization $\langle S\rangle_0$ may all be periodic functions of time.

The resonant frequency of the system is $\omega_0 = \gamma H_0$. If

$$\langle \vec{S} \rangle' = \langle S \rangle_x' \hat{x} + \langle S \rangle_y' \hat{y} + \langle S \rangle_z' \hat{z} \tag{12}$$

is a time-dependent solution of Eq. (11) at the frequency $\omega = \omega_0 + \delta$, then a straightforward substitution shows that the solution at the frequency $\omega = \omega_0 - \delta$ is

$$\langle \vec{S}(t) \rangle'' = \langle S \rangle_x' \hat{x} - \langle S \rangle_y' \hat{y} + \langle S \rangle_z' \hat{z} . \tag{13}$$

Thus, as long as the atoms obey Bloch's equations and the detection method is sensitive to the z components of $\langle \vec{S} \rangle$, the line shape is symmetric about ω_0 and a pulsed discharge will not shift the center frequency of the line shape. Moreover, experimental evidence, discussed in Sec. V, shows that the pulsed discharge does not shift the Zeeman resonances.

C. ^{4}He(2^3S_1) Zeeman linewidth

The estimated contributions to the ^{4}He(2^3S_1) Zeeman linewidth are listed in Table I for the four different pressure sample cells. Those in the upper half of the table will be present even in the late afterglow of a discharge, while those in the lower half of the table are due to the discharge. The total estimated linewidth may be compared with the narrowest observed linewidth which is listed on the last line. This minimum linewidth was determined by the weakest discharge which could be maintained.

Diffusion and three-body collision effects[30,31] were calculated from the measured diffusion constant Λ and the rate coefficient for the three-body reaction

$$\mathrm{He}(2^3S_1) + 2\mathrm{He} \rightarrow \mathrm{He}_2(2s^3\Sigma_u) + \mathrm{He} .$$

The conditions of our discharge were experimentally determined to be consistent with the lowest-order diffusion mode.[32] The fractional inhomogeneity in the magnetic field has been measured to be less than 1×10^{-7}. This result was used to estimate the contributions of magnetic field inhomogeneities to the helium linewidth. Traces of ^{3}He in the ^{4}He buffer gas will broaden the ^{4}He(2^3S_1) linewidth because of the coupling of the electronic spin to the ^{3}He nuclear spin. This contribution to the linewidth was estimated from the measured cross section for transfer of metastability[33] and the natural isotopic abundance of ^{3}He in ^{4}He. Note that metastability transfer between ground-state ^{4}He and ^{4}He(2^3S_1) occurring at a rate of $\approx 10^7$/sec causes no appreciable broadening of the metastable Zeeman resonance. The contribution to the helium linewidth from Penning ionization of rubidium atoms was calculated from the measured cross section[32] and the number density of rubidium atoms at 30 °C.[34] Linewidth due to energy transfer collisions with traces of neon impurities in the helium buffer gas is expected to be negligible.

The dominant contribution from the discharge products to the helium linewidth is spin-exchange collisions with free electrons. An upper limit on the number density of the free electrons in a weak discharge was obtained from a measurement of the broadening of the rubidium Zeeman resonances when the discharge was turned on. Using Eq. (1) and the known cross section for spin exchange between electrons and rubidium atoms,[35] the average number density of the free electrons was less than 1.1×10^9 cm^{-3}. Linewidth due to spin exchange with free electrons was then calculated using this number density and the cross section[36] for spin-ex-

TABLE I. Contributions to the ^{4}He(2^3S_1) linewidth.

Relaxation mechanism	Cell pressure (Torr) 5.5	7.6	8.9	13.9
Diffusion	78 Hz	56 Hz	48 Hz	31 Hz
Three-body collision	2	4	5	12
Field inhomogeneity at 100 G	28	28	28	28
(50 G)	(14)	(14)	(14)	(14)
^{3}He	10	14	16	25
Penning ionization by Rb	5	5	5	5
Spin exchange with e^-	61	61	61	61
Collision with He(2^3S_1)	7	7	7	7
Collision with He$_2$($2s\,^3\Sigma$)	10	10	10	10
Superelastic e^- collision	2	2	2	2
Total at 100 G	203	187	182	181
Minimum observed linewidth (extrapolated to zero rf power)	255 Hz	245 Hz	223 Hz	210 Hz

change collisions between electrons and $^4He(2^3S_1)$ atoms.

The other discharge products are expected to contribute less than 20 Hz to the helium linewidth. The number densities of the $He(2^3S_1)$ and He_2 molecules were estimated to be 1.5×10^{10} cm^3 and 0.7×10^{10} cm^3, respectively. The rate of destruction of $He(2^3S_1)$ atoms through collisions with $He(2^3S_1)$ atoms and He_2 molecules was calculated using the recently determined rate coefficients.[31] The cross section for the destruction of $^4He(2^3S_1)$ atoms through superelastic collisions with free electrons is[31] 4.2×10^{-16} cm^2, and this process is not expected to contribute significantly to the helium linewidth. Assuming the diffusion is ambipolar and because of other positive ions, e.g., Rb^+, the number density of He ions must be less than the number density of the free electrons. Since the velocity of these ions is a factor of 100 smaller than the electron velocity at thermal energies, charge exchange, and spin exchange with these ions are not expected to contribute significantly to the helium linewidth.

Agreement between the calculated linewidth and the minimum observed linewidth for each of the four sample cells is reasonable.

IV. PROCEDURE

Since the ^4He atom has no nuclear spin, the Hamiltonian for the 2^3S_1 state in an external magnetic field $\vec{H}_0$ is[37]

$$\mathcal{H}=g_J(^4He,2^3S_1)\,\mu_B\vec{S}\cdot\vec{H}_0\,, \tag{14}$$

where μ_B is the Bohr magneton, $\vec{S}$ is the total electronic spin, and $\vec{H}_0$ is the static magnetic field. The g_J factor is related to the Zeeman transition frequency by

$$\nu(^4He,2^3S_1)=g_J(^4He,2^3S_1)\,\mu_B H_0/h\,, \tag{15}$$

where h is Planck's constant. In the case of ^{87}Rb, the Hamiltonian is given by

$$\mathcal{H}'=g_J(^{87}Rb)\,\mu_B\vec{J}\cdot\vec{H}_0+g_I(^{87}Rb)\,\mu_B\vec{I}\cdot\vec{H}_0 + \frac{1}{I+\frac{1}{2}}\,h\Delta\nu(^{87}Rb)\vec{I}\cdot\vec{J}\,, \tag{16}$$

where $g_I(^{87}Rb)$ is the nuclear g factor, $\vec{I}$ is the nuclear spin, and $\Delta\nu(^{87}Rb)$ is the zero-field hyperfine transition frequency. The energy levels of the ground electronic state of rubidium are given by the Breit-Rabi formula[38]

$$E(F_\pm,m_F)=-\frac{h\Delta\nu}{2(2I+1)}+g_I\,\mu_B H_0 m_F \pm\frac{h\Delta\nu}{2}\left(1+\frac{4m_F x}{2I+1}+x^2\right)^{1/2}, \tag{17}$$

where

$$x=(g_J-g_I)\;\mu_B H_0/h\Delta\nu\,.$$

The symbol $F_\pm$ in this equation refers to $F=I\pm\frac{1}{2}$. The transition frequencies between adjacent Zeeman levels $(F,m_F)\rightarrow(F,m_F-1)$ are given by

$$\nu_F=g_I\,\frac{\mu_B H_0}{h}+\frac{\Delta\nu}{2}\left[\left(1+\frac{4m_F x}{2I+I}+x^2\right)^{1/2} -\left(1+\frac{4(m_F-1)x}{2I+1}+x^2\right)^{1/2}\right]. \tag{18}$$

These transition frequencies are completely determined by the three quantities $g_J(^{87}Rb)\,\mu_B H_0/h$, $g_I(^{87}Rb)/g_J(^{87}Rb)$, and $\Delta\nu(^{87}Rb)$. The ratio of the nuclear to the electronic g factor is known[18]; however, because of the hyperfine pressure shift, the zero-field hyperfine transition frequency was measured for each cell using methods described below. Then, from the measured Zeeman transition frequency, an iterative computer routine was used to find $g_J(^{87}Rb)\,\mu_B H_0/h$. Once these quantities are determined, the ratio R of the g_J factors is found:

$$R\equiv\frac{g_J(^4He,2^3S_1)}{g_J(^{87}Rb,5^2S_{1/2})}=\frac{g_J(^4He,2^3S_1)\,\mu_B H_0/h}{g_J(^{87}Rb,5^2S_{1/2})\,\mu_B H_0/h}\,. \tag{19}$$

Before any data were taken, and before the pulsed discharge was turned on, the magnetic field correction coils were adjusted for the narrowest rubidium Zeeman linewidth which was consistent with zero asymmetry in the line shape. The pulsed discharge was then turned on and allowed to stabilize for several hours. The amplitude of each resonance was usually measured at 15 different frequencies spanning at least two full linewidths. These frequencies were taken in a sequence that was chosen to minimize error due to drifts in either the magnetic field or the light intensity.

The ratio R was determined by measuring the $He(2^3S_1)$ Zeeman transition and either the $(F=2,\ m_F=2)\rightarrow(F=2,m_F=1)$ or the $(F=2,m_F=-2)\rightarrow(F=2,m_F=-1)$ transition in ^{87}Rb. The ^{87}Rb transition chosen was the one having the largest signal and depended on whether the pumping light was right or left circularly polarized. The rms error in R for a run which lasted 30 min was typically less than 1×10^{-8}. At the conclusion of one run, the light polarization was reversed, and data were taken at the opposite polarization but otherwise under the same experimental conditions. Then, to check for systematic effects, one of the experimental parameters was changed, and R was remeasured for both light polarizations.

In order to determine $g_J(^{87}Rb)$, it is necessary to know the zero-field hyperfine transition fre-

quency $\Delta\nu$ for each cell. The fractional shift in $\Delta\nu$ with helium pressure is[39]

$$\frac{1}{\Delta\nu}\frac{\partial\Delta\nu}{\partial p} = +(1.05\pm0.02)\times 10^{-7}/\mathrm{Torr(He)}.$$

Measuring $\Delta\nu$ also provided a convenient and accurate method of determining the helium pressure. Experimental determinations of one of the Zeeman transition frequencies, one of the hyperfine transition frequencies, and a knowledge of $g_I(^{87}\mathrm{Rb})/g_J(^{87}\mathrm{Rb})$ uniquely determines $\Delta\nu$ via an iterative computer routine. There was no observable shift in the Rb hyperfine transition when the discharge was turned on.

V. RESULTS

A. Pumping light effects

The difference between determinations of R for the two light polarizations was typically 1×10^{-7} at full light intensity in a 100-G magnetic field. Figure 3 shows the results for three different light intensities. In this case, the 8.9-Torr cell was used at a magnetic field of 50 G. To within the experimental accuracy, the average value of R for the two light polarizations is independent of the intensity of the rubidium pumping light. Measurements similar to these were repeated for all four sample cells at magnetic fields of 50 and 100 G under a wide variety of discharge conditions. In addition, the direction of the static magnetic field was reversed with respect to the direction of the incident light. The averaged values of R were consistently independent of the light intensity. Therefore, under any given set of experimental conditions, it was unnecessary to extrapolate all data to zero light intensity.

To determine what portion of this difference in the ratios of the g_J factors was due to a ^{87}Rb shift and what portion was due to a ^{4}He shift, each atom's g_J factor was measured at both light polarizations. The observed ^{4}He g_J factor shift was the same order of magnitude as the rms error in R for any one given run, and therefore, was taken to be independent of the polarization of the light.

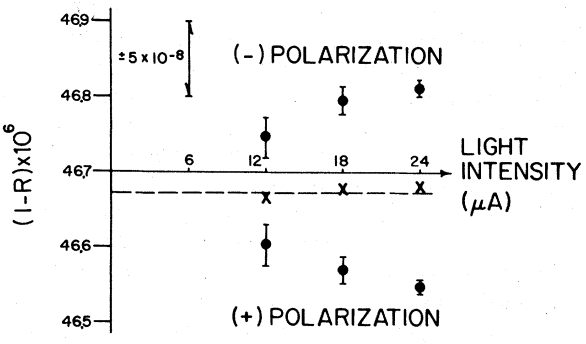

FIG. 3. Change in $R=g_J(^4\mathrm{He},2^3S_1)/g_J(^{87}\mathrm{Rb},5^2S_{1/2})$ with intensity and polarization of the Rb pumping light. The average of both polarizations is independent of light intensity.

Thus the shift in R with changes in the polarization of the light was due to rubidium, and the shift of the Rb g_J factor was smaller when the discharge was off than when the discharge was on. In one case at full light intensity, the shift at 100 G was $(5.6\pm0.5)\times10^{-8}$ with the discharge off and $(8.1\pm0.5)\times10^{-8}$ with the discharge on. An additional feature of this shift in the effective ^{87}Rb g_J factor was proportionality to the light intensity, but only when the discharge was off.

The observed shift may be explained by the combined effect of the pumping light and spin-exchange collisions with free electrons. Any shift in the effective g_J factor due to the pumping light is proportional to the intensity of the light. Barrat and Cohen-Tannoudji[40] pointed out that light shifts may arise from either real or virtual transitions to the excited state. Bulos, Marshall, and Happer[41] have shown that there is no light shift due to real transitions for the Zeeman transitions we observe at each light polarization. Also, Mathur, Tang, and Happer[42] have shown that in the low-field limit, the light shift due to virtual transitions moves the transition frequencies equal amounts in opposite directions for the transitions we observe. The shift in the ^{87}Rb g_J factor with the discharge off is attributed to virtual light transitions.

The additional shift when the discharge is on can be accounted for through the effects of spin-exchange collisions with free electrons. From Eq. (3), the ratio of the shift in the ^{87}Rb Zeeman transition frequency, $\delta\nu_{\mathrm{Rb}}$, to that part of the rubidium linewidth due to spin-exchange collisions with free electrons for either of the observed transitions is

$$\delta\nu_{\mathrm{Rb}}/\Delta f_{\mathrm{Rb}} = \tfrac{1}{5}KP(e).$$

Both the intensity and polarization of the pumping light will change $\delta\nu_{\mathrm{Rb}}$ since the electron polarization will change. Although this effect is expected to increase with increasing light intensity, it is not proportional to the light intensity.

The above relation may be used to estimate the electron polarization in our sample cell. A recent measurement[43] of the constant K at room temperature gave

$$K = 0.75\pm0.38.$$

For a discharge of moderate intensity, a typical shift in the ^{87}Rb g_J factor not due directly to light was 0.88 ± 0.21 Hz. Using these values,

$$\Delta f_{\mathrm{Rb}}P(e) = 5.9\pm3.3\ \mathrm{Hz}.$$

If, out of the total rubidium resonance linewidth of 280 Hz, the contribution of spin exchange with electrons is taken as 150 Hz, for example, then the electron polarization is $(3.9 \pm 2.2)\%$.

B. Line shape

The measured signal amplitudes for the rubidium and helium resonances were fitted to a Lorentzian line shape having the form

$$F_1(\omega) = B + A\Gamma^2/[\Gamma^2 + (\omega - \omega_0)^2] \,, \tag{20}$$

where ω_0 is the resonant frequency, 2Γ is the linewidth, A is the signal amplitude at resonance, and B is a constant baseline. The procedure used to determine these constants was a χ-squared minimization routine. The center frequencies of these resonances were then used to determine the $g_J \mu_B H/h$ product for each atom.

Any possible asymmetry in the rubidium and helium line shapes was examined in two different ways. First, the data for both resonances were refitted to a line shape having the form

$$F_2(\omega) = B + \frac{A[\Gamma^2 + 4\xi(\omega - \omega_0)]}{\Gamma^2 + (\omega - \omega_0)^2} \,, \tag{21}$$

where ξ is an asymmetry parameter. Using this line shape, no consistent asymmetry was found in the rubidium line shape; typical values of ξ were less than 0.1 Hz, and the sign might change from one run to the next. However, the helium line shape was consistently found to be slightly asymmetric with $\xi = +5$ Hz. This observed asymmetry led us to pursue another method of measuring its magnitude.

As discussed in Sec. III, the effects of transfer of coherence in spin-exchange collisions between free electrons and metastable helium atoms shifts the center frequency of each resonance and introduces an asymmetry in the line shape. Since the amplitude of the electron resonance was so small that it was barely observable for the conditions under which we took data, the expected line shape is given by Eq. (10). This line shape may be rewritten in the form

$$F_3(\omega) = B + \frac{A'\Gamma^2[1 + \alpha(\omega - \omega_0)/\Gamma_0]}{(\omega - \omega_0)^2 + \Gamma_0^2 + (\Gamma^2 - \Gamma_0^2)[1 + \alpha(\omega - \omega_0)/\Gamma_0]} \,, \tag{22}$$

where

$$\Gamma_0 = 1/T'_{2h} \,, \quad \omega_0 = \omega'_{0h} \,,$$
$$\alpha = B_4/B_3 \,, \quad A' = A(\Gamma^2 - \Gamma_0^2)/\Gamma^2 \,.$$

If the linewidth at zero rf power, Γ_0 is known, the other parameters may be determined by fitting the data to this line shape. In practice, the line shape was measured at several different rf power levels, and the approximate linewidth was determined using Eq. (20) as the fitting function. These linewidths were then extrapolated to zero rf power to find Γ_0. This value of Γ_0 was then used when fitting the data to the line shape given in Eq. (22).

Figure 4 shows the measured data points for a helium resonance. The solid line is the fitted Lorentzian line shape with no provision made for the asymmetry in the line shape. The error bar on one of the data points indicates the rms error in the signal amplitude. This figure shows that the asymmetry in the line shape is very small.

Figure 5 is a comparison of R's determined using the Lorentzian line shape given by Eq. (20) and the modified Lorentzian line shape given by Eq. (22). The difference between the two methods of determining R was about 2×10^{-8}. As shown in the figure, this difference decreases with decreasing values of the helium linewidth.

At a magnetic field of 100 G, typical values of the asymmetry parameter α indicate that the amplitude of the dispersion signal was $\frac{1}{50}$ of the amplitude of the Lorentzian part of the signal. It is difficult to calculate α, since the relaxation times and the sensitivity of the detection method

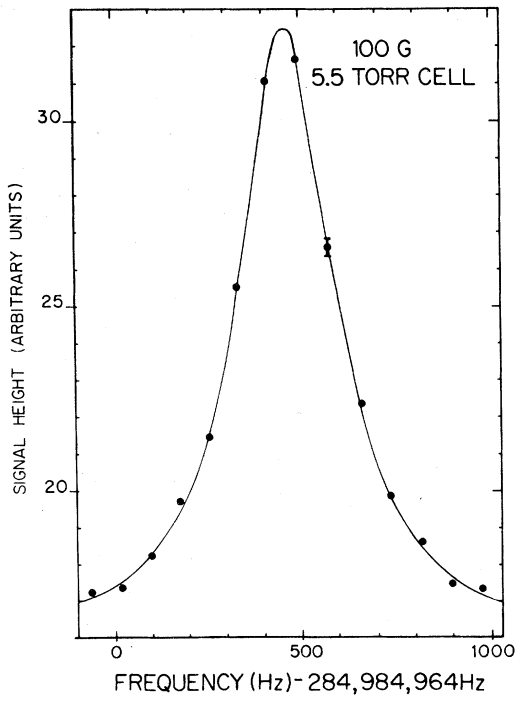

FIG. 4. Helium 2^3S_1 Zeeman resonance at 100 G. A typical error is shown for one of the data points, which were taken alternately on opposite sides of the resonance. The solid curve is a fitted Lorentzian line shape.

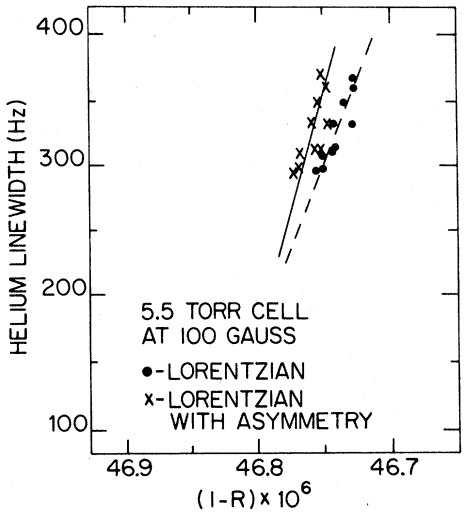

FIG. 5. Discharge intensity vs $R = g_J(^4\mathrm{He}, 2^3S_1)/g_J(^{87}\mathrm{Rb}, 5^2S_{1/2})$. The experimental value for R has a linear dependence on the linewidth of the helium resonance, which serves as an indication of the discharge intensity. Results are shown for both a Lorentzian line shape and a Lorentzian-plus-asymmetry fit to the $\mathrm{He}(2^3S_1)$ resonance.

to the electron and helium polarizations were not all known. However, assuming that the detection method is only sensitive to the electron polarization, an approximate calculation shows that the observed values of the asymmetry are reasonable.

C. Discharge effects

After corrections had been made in R for the effects due to light polarization, and asymmetry in the helium line shape, we observed an empirical linear relation between the measured value of R and the $^4\mathrm{He}(2^3S_1)$ Zeeman resonance linewidth. Changes in this linewidth could be effected by changes in the rf-discharge parameters: pulse-width, pulse frequency, or amplitude of the rf. A comparison of the g_J factors obtained at different discharge intensities showed that the dominant contribution to a change in R was a shift in the $^4\mathrm{He}(2^3S_1)$ Zeeman transition. Whenever the discharge intensity, as measured by observed linewidth, was increased, this resonance shifted toward higher frequencies (in the direction of the free-electron Zeeman resonance).

After neutron irradiation of the cells, the change in R for a given change in the helium linewidth was smaller in the 8.9- and 13.9-Torr cells. For the sample cells filled with 5.5 and 7.6 Torr of helium buffer gas, the linewidths of the helium Zeeman resonance after irradiation were not noticeably narrower, and the change in R for a given change in the helium linewidth was not significantly smaller. The zero-field rubidium hyperfine transition frequency was remeasured after irradiation in the 13.9-Torr cell to see if the pressure had changed. The change, if any, was less than 0.2 Torr. Only data taken after irradiation of the sample cells were used to determine the R's given in the conclusion of this paper.

Data taken in the 8.9-Torr sample cell at magnetic fields of 50 and 100 G are shown in Fig. 6. The center frequency was determined using fits to a Lorentzian line shape. The solid lines are least-squares straight-line fits to the data. The experimental errors for the data taken at a magnetic field of 100 G were consistently less than $\pm 1 \times 10^{-8}$ and in many cases were on the order of $\pm 3 \times 10^{-9}$; the change in R with increasing discharge intensity was considerably larger. Data taken in the 5.5-, 7.6-, and 13.9-Torr sample cells showed similar changes in R with increasing helium linewidth.

For each cell, the rf power was varied to determine if it contributed to the change in R. For a magnetic field of 100 G, the effects of asymmetry in the line shape were removed using the line shape given by Eq. (22). Then, the only effect of an increase in the rf power was a broadening of the helium line shape. However, when a Lorentzian line shape was used to determine the center frequency of the helium resonance at a magnetic field of 50 G, an increase in the rf power produced an observable change in R.

The rubidium vapor pressure is a sensitive function of the temperature of the sample cell. To check for effects of the rubidium density on R, measurements were made in the 13.9-Torr cell at a field of 100 G at temperatures from 24.6 to 34.0 °C. This changes the rubidium density by more than a factor of 3.[34] If the shift in the helium Zeeman frequency is caused by collisions with rubidium atoms, then there should be a significant increase in this shift. Within the experimental error of approximately 2×10^{-8}, no change in R was observed. The discharge parameters were kept constant as the temperature was changed.

The effects of transfer of coherence in spin-exchange collisions between free electrons and $^4\mathrm{He}(2^3S_1)$ atoms qualitatively explained many of the features observed in this experiment. The helium resonance was consistently observed to be slightly higher on the side of the electron resonance, and the electron resonance was observed to be higher on the side of the helium resonance. As the intensity of the discharge was increased, the center frequency of the helium reso-

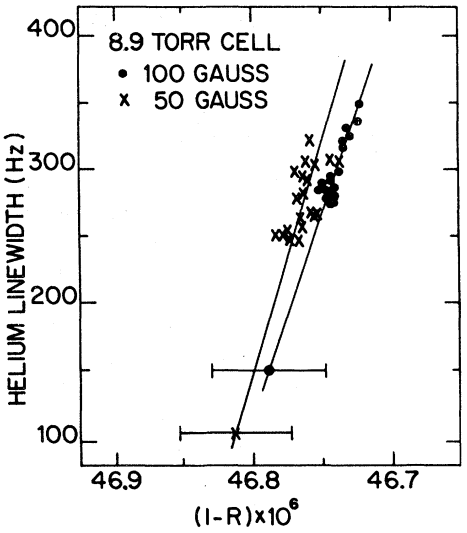

FIG. 6. Discharge intensity vs $R = g_J(^4\mathrm{He}, 2^3S_1)/g_J(^{87}\mathrm{Rb}, 5^2S_{1/2})$. Results for R at both 50 and 100 G depend upon the linewidth of the He (2^3S_1) resonance, which has been fit using a Lorentzian line shape. The final value for R is obtained by extrapolating to the helium linewidth expected at zero discharge intensity. The determination of the error is discussed in Sec. V.

nance consistently moved toward higher frequencies (in the direction of the electron resonance). The width of the electron resonance and its comparatively poor signal-to-noise ratio prohibited observation of equivalent shifts in the electron resonance.

A rigorous limit on the shift in the helium or electron center frequency due to transfer of coherence in spin-exchange collisions may be derived by requiring that the contribution of spin exchange to the electron and helium linewidths and the other known contributions to the linewidths be less than the observed linewidths. This limit is independent of the cross section for spin-exchange collisions. Before the sample cells were irradiated, the observed change in R was 30% larger than the limit on the change due to transfer of coherence in spin-exchange collisions. After irradiation of the cells, the observed change was still slightly larger than predicted. This result indicates that there may be additional processes which contribute to the shift in the $^4\mathrm{He}(2^3S_1)$ center frequency.

D. Determination of R

The systematic change in R with discharge intensity is clearly the limiting factor in the accuracy of this experiment. While the rms error in the measured value of R under a given set of experimental conditions was as small as several parts in 10^{-9}, a change of several parts in 10^{-8} occurred when an increase in discharge intensity caused the helium linewidth to increase by 100 Hz. The method used to determine the final experimental value of R and its error is now described.

An extrapolation toward smaller values of the helium linewidth is necessary: first, a least-squares linear fit to the data consistently showed that R decreased with increasing helium linewidth. Secondly, it was shown above that the contribution of the asymmetry in the helium linewidth to the change in R was reduced at smaller values of the helium linewidth. Finally, such an extrapolation procedure tends to remove the effects of transfer of coherence in spin-exchange collisions.

The method used to extrapolate R follows: using R values determined from a Lorentzian line-shape fitting function, a least-squares straight-line fit was made to R versus helium linewidth. This was done for each of the four sample cells at magnetic fields of 50 and 100 G. The extrapolation was terminated at the calculated value of the helium linewidth in the absence of a discharge; see Table I. Included were contributions from diffusion, three-body collisions, inhomogeneities in the magnetic field, collisions with ^{3}He, and Penning ionization by Rb. The increase of linewidth due to rf power broadening was also included. The results are summarized in Fig. 7. Because of the uncertainty in this extrapolation procedure, the error-bar half-sizes were taken to be equal to the difference between R at the smallest observed helium

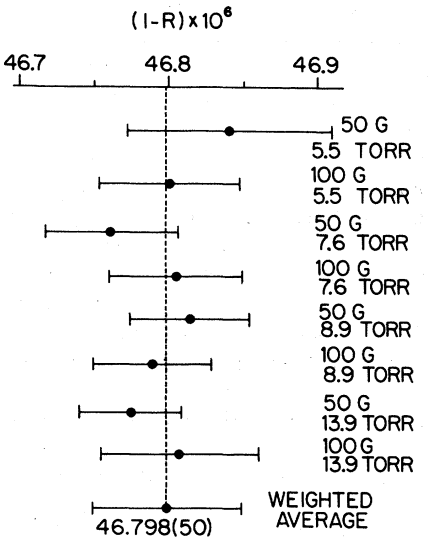

FIG. 7. Summary of the final extrapolated values of $R = g_J(^4\mathrm{He}, 2^3S_1)/g_J(^{87}\mathrm{Rb}, 5^2S_{1/2})$ for the four sample cells at both 50 and 100 G.

linewidth and the extrapolated value of R. (See Fig. 6.)

The final value of R is the average over all cells at both values of the magnetic field. The result is

$$R \equiv \frac{g_J(^4\mathrm{He}, 2^3S_1)}{g_J(^{87}\mathrm{Rb}, 5^2S_{1/2})} = 1 - 46.798(50) \times 10^{-6}.$$

The error of $\pm 5 \times 10^{-8}$ was chosen to include all the extrapolated values of the g_J-factor ratio. The rms error is considerably smaller.

E. Other systematic errors

We considered a number of effects which could contribute to possible systematic errors in R. In every case, the extrapolation procedure described above would tend to remove these effects, or we were able to show that the error was much smaller than the error given above.

1. Presence of other signals

Our preliminary investigations of the shift in the helium 2^3S_1 center frequency with discharge intensity focused on finding out how much the nearby electron resonance line could perturb the helium line shape. With the observed signal amplitudes, center frequencies, and linewidths, a computer program was used to find the shift in the helium resonance caused by the proximity of the electron resonance, i.e., the effect of one Lorentzian resonance overlapping another. We found that this overlap could contribute less than 10% of the observed shift in the helium resonance at a 50-G magnetic field. At a 100-G magnetic field the two resonances were well resolved and the contribution of the electron resonance to the observed shift in the helium resonance is negligible due to the overlap effect. In addition, the extrapolation procedure described above would tend to remove these effects.

Henry and Silver[44] have shown that the Zeeman transition frequency in a magnetic field is decreased by relativistic time dilation and Thomas precession. The electrons created in a collision between two metastable helium atoms have an energy centered around 15.1 eV. In a 50-G magnetic field, the Zeeman resonance for such hot electrons, if observable in our experiment, would lie 1.6 kHz above the $^4\mathrm{He}(2^3S_1)$ Zeeman resonance while the Zeeman resonance for thermal electrons lies 5.7 kHz above the helium resonance. If the electron resonance is shifted closer to the helium resonance, the effects of transfer of coherence in spin-exchange collisions will be increased. However, for those cases where the free-electron Zeeman resonance was determined by using ≥ 10 dB more power than normal, the resonant frequency implied thermal electrons. Again, the extrapolation procedure described above would tend to correct for these effects.

2. Magnetic field inhomogeneities

Inhomogeneities in the magnetic field may shift the measured value of R. Such effects were studied by adjusting the magnetic field correction coils, measuring R, readjusting the correction coils, and remeasuring R. We found that after readjustment, consistency to within a fractional error of $\pm 1 \times 10^{-8}$ was obtained. In addition, readjustments were made many times during the experiment. This would tend to cancel any shifts due to magnetic field inhomogeneities.

3. Bloch-Siegert shift

The simultaneous application of rf magnetic fields oscillating at two different frequencies may cause a shift in the magnetic-resonance signal.[45,46] In our case, such an effect is possible if the rf oscillator used to drive the discharge operates at a frequency which lies too close to the rubidium Zeeman frequency. This shift was observed in the $(F=2, m_F=2) \longleftrightarrow (F=2, m_F=1)$ ^{87}Rb transition at 69 MHz when the discharge oscillator was purposely tuned near this frequency. However, no shift was found in the $^{87}\mathrm{Rb}(F=2, m_F=-2) \longleftrightarrow (F=2, m_F=-1)$ transition at 74 MHz. A separation of 5 MHz was therefore sufficient to make the effect insignificant. Under the usual operating conditions the frequency of the rf oscillator and the ^{87}Rb Zeeman frequencies were separated by about 20 MHz.

4. Buffer gas interactions

Staffa[47] has measured the fractional shift in the ^{87}Rb ground-state g_J factor due to interactions with a helium buffer gas. For pressures used in our experiment, this effect is negligible. Similar shifts in the $^4\mathrm{He}(2^3S_1)$ g_J factor due to spin-orbit coupling in collisions with ground-state helium atoms have not been measured, but there was no observed dependence of R on the helium buffer gas pressure.

5. Incorrect values of $\Delta\nu(^{87}Rb)$ and $g_I(^{87}Rb)/g_J(^{87}Rb)$

Two possible additional sources of systematic error in this experiment are errors in the zero-field hyperfine transition frequency, $\Delta\nu(^{87}\mathrm{Rb})$, and the g_I/g_J ratio for the ground state of rubidium. These values are required by the program which uses the Breit-Rabi equation to determine the g_J factor. A fractional error of 6×10^{-6} in g_I/g_J is required to produce a fractional shift of 1×10^{-8} in the g_J factor. However, this ratio has been mea-

sured[18] to a fractional accuracy of 0.9×10^{-6}. Similarly, a fractional shift of 1×10^{-8} in the g_J factor requires the zero-field hyperfine transition frequency to be in error by 2.1 kHz out of 6.83 GHz. The zero-field hyperfine transition frequency was easily measured to within 100 Hz for each sample cell used. Furthermore, to first order, any error in this frequency will produce equal and opposite shifts in the g_J factor determined by measuring the $(F=2, m_F=2) \leftrightarrow (F=2, m_F=1)$ and the $(F=2, m_F=-1) \leftrightarrow (F=2, m_F=-2)$ transitions. Since these g_J factors were averaged to correct for shifts due to the polarization and intensity of the light, any error in the zero-field hyperfine transition frequency will give a very small error in R. At the level of accuracy obtainable in this experiment, the contributions of errors in $\Delta\nu(^{87}\mathrm{Rb})$ and $g_I(^{87}\mathrm{Rb})/g_J(^{87}\mathrm{Rb})$ are insignificant.

VI. CONCLUSION

Our final experimental result is

$$R \equiv \frac{g_J(^4\mathrm{He}, 2^3S_1)}{g_J(^{87}\mathrm{Rb}, 5^2S_{1/2})} = 1 - 46.798(50) \times 10^{-6}.$$

Using the previously determined ratio of the g_J factor of the ground state of ^{87}Rb to the g_J factor of hydrogen,[7] we find

$$\left.\frac{g_J(^4\mathrm{He}, 2^3S_1)}{g_J(^1\mathrm{H}, 1^2S_{1/2})}\right|_{\text{expt.}} = 1 - 23.214(50) \times 10^{-6}.$$

This result agrees with the theoretical calculation of Grotch and Hegstrom, and Barkley and Hegstrom[9]:

$$\left.\frac{g_J(^4\mathrm{He}, 2^3S_1)}{g_J(^1\mathrm{H}, 1^2S_{1/2})}\right|_{\text{theory}} = 1 - 23.211 \times 10^{-6}.$$

The error in our experimental result is slightly smaller than the bound state corrections to the Schwinger moment.[16]

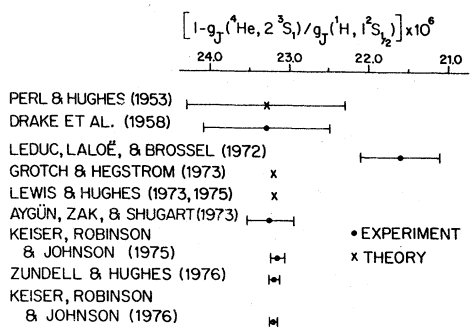

FIG. 8. Summary of the theoretical and experimental values for $g_J(^4\mathrm{He}, 2^3S_1)$.

This experimental result is compared with earlier experimental and theoretical results in Fig. 8. The crosses in this figure represent theoretical calculations while the circles represent experimental values. This figure includes a preliminary result for this experiment[10] as well as this final result. Our experiment agrees with the experimental values obtained using an atomic beam technique,[17,48] but disagrees with another value obtained using an optical-pumping technique.[13]

ACKNOWLEDGMENTS

We would like to thank Dr. Fred Steinkruger and the staff of the North Carolina State University nuclear reactor for their assistance with the neutron irradiation of the sample cells. In addition, we appreciate the glass-blowing assistance of Stanley Mezynski at North Carolina State and Thomas A. Henson at Duke. We would also like to thank Professor Will Happer for useful discussions concerning the transfer of coherence during spin-exchange collisions.

---

‡Work supported in part by the NSF under Grant No. MPS 75-14065.

†Present address: Joint Institute for Laboratory Astrophysics, Univ. of Colorado, Boulder, Colo. 80309.

[1]F. G. Walther, W. D. Phillips, and D. Kleppner, Phys. Rev. Lett. 28, 1159 (1972).
[2]J. S. Tiedeman and H. G. Robinson, *Atomic Physics 3*, edited by S. J. Smith and G. K. Walters (Plenum, New York, 1973), p. 85.
[3]R. A. Hegstrom, Phys. Rev. A 11, 421 (1975).
[4]V. Beltran-Lopez, E. Blaisten, N. Segovia, and E. Ley Koo, Phys. Rev. 177, 432 (1969).
[5]V. Beltran-Lopez and T. Gonzalez, Phys. Rev. A 2, 1651 (1970).
[6]C. L. Pekeris, Phys. Rev. 115, 1216 (1959).
[7]W. M. Hughes and H. G. Robinson, Phys. Rev. Lett. 23, 1209 (1969).
[8]M. L. Lewis and V. W. Hughes, Phys. Rev. A 8, 2845 (1973); Phys. Rev. A 11, 383 (1975).
[9]H. Grotch and R. A. Hegstrom, Phys. Rev. A 8, 1166 (1973); P. G. Barkley and R. A. Hegstrom, Phys. Rev. A 14, 1574 (1976).
[10]G. M. Keiser, H. G. Robinson, and C. E. Johnson, Phys. Rev. Lett. 35, 1223 (1975).
[11]C. W. Drake, V. W. Hughes, A. Lurio, and J. A. White, Phys. Rev. 112, 1627 (1958).
[12]W. Perl and V. Hughes, Phys. Rev. 91, 842 (1953).
[13]M. Leduc, F. Laloë, and J. Brossel, J. Phys. (Paris) 33, 49 (1972).
[14]P. F. Winkler, D. Kleppner, T. Myint, and F. G. Walther, Phys. Rev. A 5, 83 (1972).
[15]W. L. Williams and V. W. Hughes, Phys. Rev. 185, 1251 (1969).
[16]R. A. Hegstrom (private communication).

[17]E. Aygün, B. D. Zak, and H. A. Shugart, Phys. Rev. Lett. 31, 803 (1973).
[18]C. W. White, W. M. Hughes, G. S. Hayne, and H. G. Robinson, Phys. Rev. 174, 23 (1968).
[19]S. F. Watanabe, thesis (Duke University, 1972) (unpublished).
[20]J. S. Tiedeman, thesis (Duke University, 1974) (unpublished).
[21]P. A. Franken and F. D. Colegrove, Phys. Rev. Lett. 1, 316 (1958).
[22]L. D. Schearer, Phys. Rev. A 10, 1380 (1974).
[23]L. C. Balling, R. J. Hanson, and F. M. Pipkin, Phys. Rev. 133, A607 (1964).
[24]F. Grossetête, J. Phys. (Paris) 25, 383 (1964).
[25]F. Grossetête, J. Phys. (Paris) 29, 456 (1968).
[26]W. Happer and H. Tang, Phys. Rev. Lett. 31, 273 (1973).
[27]J. Dupont-Roc, M. Leduc, and F. Laloë, J. Phys. (Paris) 34, 977 (1973).
[28]G. M. Keiser, thesis (Duke University, 1976) (unpublished).
[29]F. Bloch, Phys. Rev. 70, 460 (1946).
[30]A. V. Phelps and J. P. Molnar, Phys. Rev. 89, 1202 (1953).
[31]R. Deloche, P. Monchicourt, M. Cheret, and F. Lambert, Phys. Rev. A 13, 1140 (1976).
[32]C. E. Johnson, C. A. Tipton, and H. G. Robinson (to be published).
[33]J. Dupont-Roc, M. Leduc, and F. Laloë, Phys. Rev. Lett. 27, 467 (1971).
[34]A. Gallagher and E. L. Lewis, J. Opt. Soc. Am. 63, 864 (1973).
[35]S. J. Davis and L. C. Balling, Phys. Rev. A 6, 1479 (1972).
[36]L. D. Schearer, Phys. Rev. 171, 81 (1968). The value for the cross section in this reference has been multiplied by 2 because of a difference in definition.
[37]The sign convention for the g factor is that of P. Kusch and V. W. Hughes, in *Encyclopedia of Physics*, Vol. 37, edited by S. Flugge (Springer-Verlag, Berlin, 1959).
[38]G. Breit and I. I. Rabi, Phys. Rev. 38, 2082 (1931).
[39]P. L. Bender, E. C. Beaty, and A. R. Chi, Phys. Rev. Lett. 1, 311 (1958).
[40]J. P. Barrat and C. Cohen-Tannoudji, J. Phys. Radium 22, 443 (1961).
[41]B. R. Bulos, A. Marshall, and W. Happer, Phys. Rev. A 4, 51 (1971).
[42]B. S. Mathur, H. Tang, and W. Happer, Phys. Rev. 171, 11 (1968).
[43]S. J. Davis and L. C. Balling, Phys. Rev. A 8, 1136 (1976).
[44]G. R. Henry and J. E. Silver, Phys. Rev. 180, 1262 (1969).
[45]F. Bloch and A. Siegert, Phys. Rev. 57, 522 (1940).
[46]N. F. Ramsey, *Molecular Beams* (Oxford U. P., London, 1956), p. 122.
[47]N. F. Staffa, thesis (Duke University, 1973) (unpublished).
[48]B. E. Zundell and V. W. Hughes, Phys. Lett. A 59, 381 (1976).